

Spin-glass formation and development of ferromagnetism in the iron-nickel-chromium system

V. I. Gorman'kov, B. N. Tret'yakov, and V. I. Kleĭnerman

I. P. Bardin Central Research Institute of Ferrous Metallurgy

(Submitted 20 November 1984)

Zh. Eksp. Teor. Fiz. **88**, 1827–1833 (May 1985)

Magnetic neutron-diffraction methods and measurements of the magnetic susceptibility have yielded the magnetic structure and spin-glass parameters at various transition concentrations in high-density system. A ferro-antiferromagnetic transformation was observed in the $\text{Fe}_{70}\text{Ni}_{30-x}\text{Cr}_x$ system with all the transitions accompanied by subcritical magnetic scattering of the neutrons at low temperatures. The diagrams of the magnetic states are constructed and it is found that the spin glass is produced by a cluster mechanism. The spin-glass "freezing" temperature is found to depend on the adjacent magnetic states, and the evolution of the ferromagnetic order is found to be similar to that of percolation.

INTRODUCTION

The magnetic state known as spin glass, which of late has been extensively investigated,¹ is the result of competing exchange interactions that occur in both dilute and high-density systems. In most cases this state precedes the establishment of long-range ferro- or antiferromagnetic order in density-dependent transitions, and is therefore being investigated near the corresponding critical concentrations c_f and c_a , where the Curie temperature T_C and the Néel temperature T_N are close to zero. Besides answering questions concerning the formation of the long-range orders, it becomes necessary to ascertain the influence of adjacent states on the spin-glass formation and to classify the resulting spin glass.² The Fe–Ni–Cr ternary system, in which three types of magnetic phase transition can occur, is therefore favorable for studying spin glass formation and the development of ferromagnetic long-range order.

Small-angle magnetic scattering of neutrons (SMSN), which accompanies spin-glass formation, was observed earlier³ in $\text{Fe}_{65}\text{Ni}_{35-x}\text{Cr}_x$ compounds, and the feasibility of formation of cluster spin glass was suggested in Ref. 4 on the basis of magnetic measurements. Investigations⁵ of $(\text{Fe}_x\text{Ni}_{80-x})\text{Cr}_{20}$ permitted a partial construction of the magnetic-states diagram and led to the rather paradoxical conclusion that the spin-glass "freezing" temperature T_g is independent of the mechanism of spin-glass formation.

We report here that the results of joint neutron-diffraction and magnetic investigations of three quasibinary systems $\text{Fe}_{55}\text{Ni}_{45-x}\text{Cr}_x$, $\text{Fe}_{65}\text{Ni}_{35-x}\text{Cr}_x$ and $\text{Fe}_{70}\text{Ni}_{30-x}\text{Cr}_x$, for which the onset of spin glass and the evolution of ferromagnetism is tracked in concentration-dependent transitions from the paramagnetic state and from states with short- and long-range antiferromagnetic orders, respectively. The measurements of these solid solutions cover thus four different states that participate in the formation of spin glass.

I. TECHNIQUE AND SAMPLES

Long-range antiferromagnetic order was investigated at 4.2 K with a neutron diffractometer at the output wavelength $\lambda = 1.19 \text{ \AA}$ of a germanium monochromator; this

procedure eliminated contributions from neutrons with $\lambda/2$.

The SMSN cross sections $d\sigma/d\Omega$ were measured with a $\lambda = 1.94 \text{ \AA}$ diffractometer at 4.2 K in the range $0.04 \leq q = 4\pi \sin \theta / \lambda \leq 0.3$. The SMSN intensities were separated either by subtracting the intensities of an iron-nickel standard in which no SMSN took place, or by subtracting the temperature-dependent part of the SMSN after heating the sample high above T_C .³

From the temperature dependences of the SMSN intensities at $q = 0.04 \text{ \AA}^{-1}$ one can determine T_C accurately enough, but the estimated values of T_g are apparently beyond the resolving power of the apparatus.⁶

To determine T_g , as well as to estimate T_N and T_C by various methods, we measured the temperature dependences of the magnetic susceptibilities χ . The values of χ measured by the Faraday method change near c_f by almost three orders, and to obtain the required accuracy it was necessary to vary the polarizing magnetic field in the course of the measurements from 100 to 1000 Oe.

The temperature dependences of the differential magnetic susceptibility χ_{ac} were obtained with a differential transformer at frequencies 200–500 Hz in a 0.5 Oe field.

The samples for the neutron-diffraction measurements were polycrystalline cylinders 8 mm in diameter and 70 mm long. The samples were quenched in water after annealing at 1273 K for 24 h, and had a single-phase fcc structure. The samples for the measurements of χ were cut from these cylinders. The sample compositions are marked on the figures.

II. MAGNETIC SCATTERING OF NEUTRONS AND MAGNETIC SUSCEPTIBILITY

1. Long-range antiferromagnetic order. The $\text{Fe}_{70}\text{Ni}_{30-x}\text{Cr}_x$ alloys require a special neutron-diffraction study of their long-range antiferromagnetic order, as well as location of the ferro-antiferromagnetic transition point, since only one composition of these alloys is known, with $T_N = 26 \pm 1 \text{ K}$ (Ref. 7).

Neutron-diffraction patterns obtained from samples with $c_{\text{Ni}} = 14.9\%$ and $c_{\text{Ni}} = 17.5\%$ (the percentages are atomic throughout) at 4.2 K contain antiferromagnetic (110) reflections,⁷ from whose intensities the average mag-

netic moments per sublattice are estimated. Assuming a collinear atomic structure, they are equal to $\mu_a = 0.48 \pm 0.05\mu_B$ and $\mu_b = 0.43 \pm 0.05\mu_B$, respectively, in good agreement with the results of Ref. 7.

The temperature dependences of the (110) peak intensities yielded respectively $T_N = 30 \pm 2$ K and $T_N = 20 \pm 2$ K, which coincide with the temperatures of the maxima of χ (see Fig. 2b below). This confirms the existence of a long-range antiferromagnetic order and of an antiferromagnetic concentration transition in the $\text{Fe}_{70}\text{Ni}_{30-x}\text{Cr}_x$ alloys.

Competing exchange interactions that cause spin glass to form are thus expected to appear in the intermediate range of compositions.

No long-range antiferromagnetic order was observed in $\text{Fe}_{65}\text{Ni}_{35-x}\text{Cr}_x$ alloys, but a short-range order with indeterminate temperature limits and the appearance of competing exchange interactions were proposed in Ref. 3 for $c_{\text{Ni}} < c_f$.

Finally, the density of the probable antiferromagnetic-order nuclei in the $\text{Fe}_{55}\text{Ni}_{45-x}\text{Cr}_x$ system is so low³ that the possible appearance of short-range order is neglected. Competing exchange interactions are made possible in this case by RKKY interaction.

2. Temperature dependences of the SMSN intensities.

Figure 1 shows the temperature dependences of the SMSN intensities of certain compositions of the $\text{Fe}_{55}\text{Ni}_{45-x}\text{Cr}_x$ and $\text{Fe}_{70}\text{Ni}_{30-x}\text{Cr}_x$ systems. Similar plots were obtained for $\text{Fe}_{65}\text{Ni}_{35-x}\text{Cr}_x$ alloys.³ It can be proposed on the basis of the analysis of Ref. 8 that this scattering is in the main quasielastic. The dependences for compositions with $c_{\text{Ni}} > c_f$ have therefore two anomalies: a critical-scattering peak at T_C and an intensity rise at low temperatures (subcritical scattering³). As the compositions shift towards c_f , the intensity becomes redistributed, decreasing at T_C and increasing at 4.2 K (Fig. 1a). The latter indicates the onset of large-scale inhomogeneities in the vicinity of c_f , and it is they which produce the subcritical scattering.

The temperatures T_0 of the start of the subcritical scattering in the systems increase successively from the paramagnetic state to the state with the long-range antiferromag-

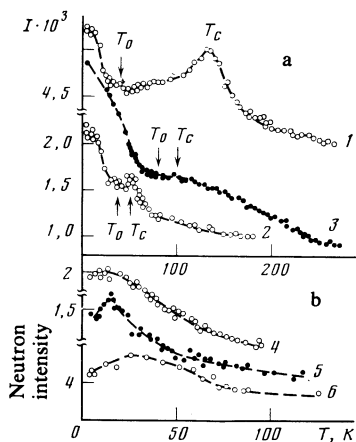


FIG. 1. Temperature dependences of the small-angle intensities I of systems at $c_{\text{Ni}} > c_f$ (a) and $c_{\text{Ni}} < c_f$ (b): $\text{Fe}_{55}\text{Ni}_{45-x}\text{Cr}_x$ —1—17.5% Cr; 2—20% Cr and $\text{Fe}_{70}\text{Ni}_{30-x}\text{Cr}_x$ —3—5% Cr; 4—7.5% Cr; 5—10% Cr; 6—12.5% Cr.

netic order (see Fig. 3 below). This increase prevents us from regarding subcritical scattering merely as scattering by finite ferromagnetic clusters,⁹ but is evidence of the influence of the magnetic states of the regions between the clusters. These regions apparently participate in the formation of the succeeding magnetic state and, in particular, of the spin-glass cluster. In Ref. 10 the subcritical scattering is also treated as an indication of development of spin glass in a ferromagnetic matrix.

Just as in Refs. 3 and 11, it is assumed that the vanishing of critical scattering attests to destruction of long-range ferromagnetic order (curve 4 of Fig. 1b); this is confirmed by magnetic measurements. These results therefore also permit an estimate of c_f .

According to Fig. 1b, magnetic inhomogeneities exist in alloys with $c_{\text{Ni}} < c_f$, and even in compositions with long-range antiferromagnetic order.

Curves 5 and 6 of Fig. 1b show respectively a local and a smeared maximum, which can be attributed to “freezing” of the spin glass. In view of the dependence of T_g on q (Ref. 6), which cannot be revealed by this procedure, these anomalies are approximate, and the values of T_g are determined from the temperature dependences of χ .

The SMSN thus offers evidence of magnetic inhomogeneities that appear near c_f and c_a and participate in the formation of both spin glass and of long-range ferromagnetic order.

3. Temperature dependences of χ . The temperature dependences of χ_{ac} of three alloys with $c_{\text{Ni}} > c_f$ and with different compositions are shown in Fig. 2a (curves 1–3). Similar plots were obtained for all the compositions investigated. Characteristic decreases of χ_{ac} with decreasing temperature are observed throughout, and are treated as “freezing” of the spin glass.^{1,2} The values of T_g are determined from the breaks on the low-temperature sides of the curves.

For compositions with $c_{\text{Ni}} < c_f$, Fig. 2 shows the temperature dependences of χ (curves 4–6). In this case, the χ traces have maxima both at T_g and T_N . The absolute values of χ and T_N , however, are smaller by 10–100 times than

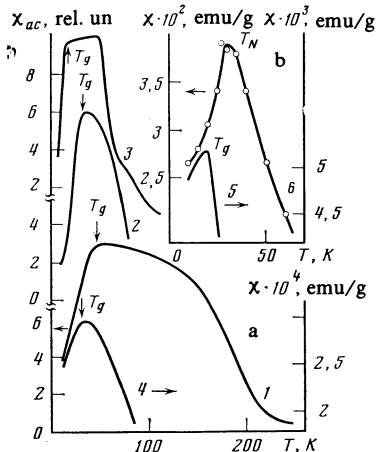


FIG. 2. Temperature dependences of the magnetic susceptibilities of the following systems: $\text{Fe}_{70}\text{Ni}_{30-x}\text{Cr}_x$ —1—5% Cr; 4—7.5% Cr; 6—14.8% Cr; $\text{Fe}_{65}\text{Ni}_{35-x}\text{Cr}_x$ —2—12.5% Cr; 5—14.7% Cr; $\text{Fe}_{55}\text{Ni}_{45-x}\text{Cr}_x$ —3—20% Cr.

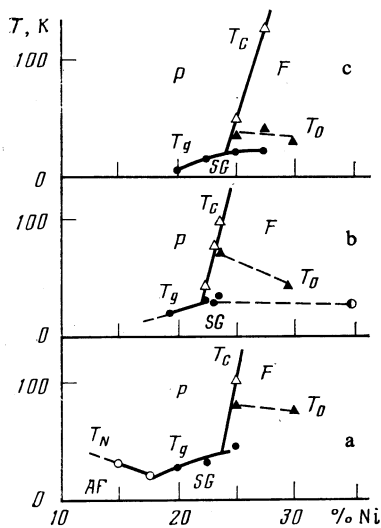


FIG. 3. Diagram of the magnetic states of the systems: (a) $\text{Fe}_{70}\text{Ni}_{30-x}\text{Cr}_x$; (b), $\text{Fe}_{65}\text{Ni}_{35-x}\text{Cr}_x$; (c) $\text{Fe}_{55}\text{Ni}_{30-x}\text{Cr}_x$. \bullet —data of Ref. 12.

those at T_g . This allows us to compare the values of T_N with the neutron-diffraction results and identify the alloys with long-range antiferromagnetic order (Fig. 2b).

4. Magnetic phase diagrams. The measured values of T_C , T_N , and T_g were used to plot in Fig. 3 the low-temperature phase diagrams. The boundaries of the long-range magnetic order were determined from a set of T_C values some of which lie outside the diagrams. The figure shows also the SMSN values of T_0 (Fig. 1a) at which “freezing” of the inhomogeneities in a ferromagnetic matrix sets in.

It follows from Fig. 3 that the concentration-dependent transitions to long-range ferromagnetic order at low temperatures are accompanied by spin-glass formation. The values of T_g increase then in succession on going from the system with the para-ferromagnetic transformation (Fig. 3c) to a system with long-range antiferromagnetic order (Fig. 3a). This growth of T_g reflects the enhancement of the competing exchange interaction responsible for the spin-glass formation. This enhancement is apparently due to the influence of the short- and long-range antiferromagnetic orders present in these adjacent states. The observed spin glass is thus an indispensable part of the adjacent states in concentration-dependent transitions.

The concentrations c_f and c_a are determined from the intersections of the T_C and T_N curves with T_g . The vanishing of the critical scattering at c_f , which can be tracked with Fig. 1a as the example, means that a topologically infinite cluster with long-range order breaks up into small finite clusters, possibly with a different value of T_C each. Therefore the concept of long-range magnetic order becomes indeterminate below T_C if $c_a < c_{\text{Ni}} < c_f$.

The substantial magnetic inhomogeneity of the alloys below T_g (Figs. 1 and 4) is, in general, evidence of the presence of two magnetic phases, a situation that can be treated also as coexistence of classical spin glass with ferro- and antiferromagnetic orders, as well as formation of randomly oriented final ferromagnetic clusters (cluster spin glass²) in ferro-, para-, and antiferromagnetic matrices.

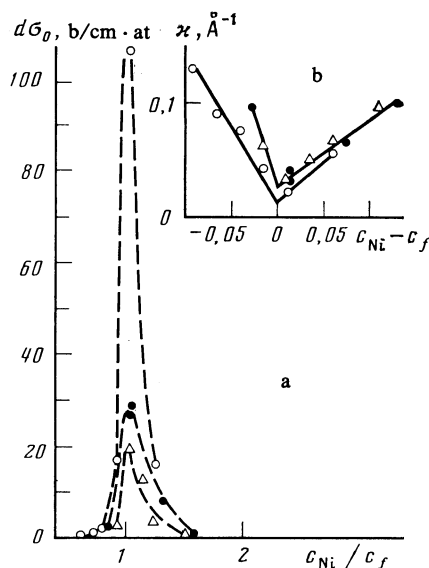


FIG. 4. Concentration dependences at 4.2 K: a—of the cross section for zero-angle magnetic neutron scattering; b—of the inverse range of magnetic correlation for the system $\text{Fe}_{70}\text{Ni}_{30-x}\text{Cr}_x$ (\circ), $\text{Fe}_{65}\text{Ni}_{35-x}\text{Cr}_x$ (\square), $\text{Fe}_{55}\text{Ni}_{45-x}\text{Cr}_x$ (\triangle).

Although T_0 and T_g are not equal, the correlation observed between them permits T_0 to be regarded as the beginning of the “freezing” of cluster spin glass. In Fig. 3b the value of T_g obtained for classical Invar $\text{Fe}_{65}\text{Ni}_{35}$ (Ref. 12) is indicated; this value agrees better with the extrapolated values of T_0 for this as well as the binary Fe–Ni system.³

III. EVOLUTION OF MAGNETIC ORDER

1. Concentration dependence of SMSN. The dependence of $d\sigma/d\Omega$ on q of the samples at 4.2 K is well described by a Lorentzian of the form

$$d\sigma/d\Omega = A / (\kappa^2 + q^2),$$

where A is the amplitude and κ is the reciprocal range of the magnetic correlation. The fact that $(d\sigma/d\Omega)^{-1}$ is linear in q^2 at $q^2 < 0.02 \text{ \AA}^{-2}$ for all alloys allows us to calculate $d\sigma_0$ at $q = 0$, as well as κ and A .

Using the analogy with thermal critical SMSN (Ref. 13) and assuming that at $T = 0$ there are no spin-density thermal fluctuations, we can write for $d\sigma/d\Omega$ (Ref. 14)

$$\frac{d\sigma}{d\Omega} = \left(\frac{\gamma e^2}{2mc^2} \right)^2 C(1-C)\chi_0(q), \quad (1)$$

where $\gamma e^2/2mc^2$ is the usual coupling constant, C is the density of the spin-density fluctuations due to composition fluctuations, and $\chi_0(q)$ is the static initial magnetic susceptibility. In turn,

$$\chi_0(q) = \frac{\chi_0(0)\kappa^2}{\kappa^2 + q^2}. \quad (2)$$

Here κ is a measure of the geometric correlation length. Since $\chi_0(0)$ diverges at c_f , a critical concentration-dependent SMSN is expected near c_f , as is in fact shown in Fig. 4.

The values of $d\sigma_0$ near c_f increase from system to system and are maximal for the ferro-antiferromagnetic transformation, thus pointing to an influence of the resulting

magnetic state in which ferromagnetism sets in and evolves. The difference between the scattering abilities is particularly pronounced at $c_{\text{Ni}} > c_f$, where short-range antiferromagnetic order obtains in the regions between finite clusters of the two systems.

The concentration dependence of κ at $c_{\text{Ni}} < c_f$ in Fig. 4b points to an increase of the magnetic-correlation length that depends on the cluster geometry and is equal to their average moment of inertia. The cluster diameters increase with increasing c_{Ni} , a topologically infinite cluster is produced at c_f , and κ should tend to zero. The κ in Fig. 4b tend to finite values that are possibly governed both by the temperature-dependent contribution and by the anisotropy of the cluster shape. Residual κ terms are observed also in temperature transformations at T_C (Ref. 11).

It can be seen that in antiferromagnetic-ferromagnetic transitions the cluster sizes turn out to be larger than the corresponding clusters of the two other systems.

The decrease of $d\sigma_0$ and the increase of κ at $c_{\text{Ni}} > c_f$ (Fig. 4) are treated in such a cluster model as a successive decrease of the share of the magnetic moments belonging to the final clusters, and to a decrease of their sizes.

The plots of the concentration dependences of A have maxima at c_f , similar to the maxima of the $d\sigma_0$ plots in Fig. 4a.

2. *Formation of cluster spin glass.* The values of $d\sigma_0$ for the $\text{Fe}_{70}\text{Ni}_{30-x}\text{Cr}_x$ system at $c_{\text{Ni}} > c_f$, shown in Fig. 4a for four compositions, are given by

$$d\sigma_0 = B(c_f - c_{\text{Ni}})^{-\gamma},$$

where $\gamma = 2.2 \pm 0.3$ is in satisfactory agreement with the values calculated in percolation theory.¹¹

The plot of κ (Fig. 4b), referred at $c_{\text{Ni}} = c_f$ to $\kappa = 0$ can be described by the relation $\kappa = (1.31 \pm 0.01)(c_f - c_{\text{Ni}})$, which presumes an exponent $\nu = 1$, close to the $\nu = 0.82$ calculated by percolation theory.¹¹

Thus, the entire behavior of the SMSN can be approximately described within the framework of percolation theory. The magnetic moments at $c_{\text{Ni}} < c_f$ are due mainly to the finite ferromagnetic clusters produced by percolation as $c_{\text{Ni}} \rightarrow c_f$. Owing to the anisotropy of the cluster shape and possibly also to the dipole interactions, the magnetic orientation of the finite clusters is random and "freezes" below T_g , thus producing cluster spin glass and causing SMSN. As c_{Ni} increases the share of the moments determined by these clusters increases, and a topologically infinite cluster is produced at c_f and determines the values of T_C and of the thermal critical SMSN.

At $c_{\text{Ni}} > c_f$, however, some of the magnetic moments continue to belong to the finite clusters separated by the non-magnetic regions, and these clusters form cluster spin glass

even in a ferromagnetic matrix. The values of κ fit well the general linear relation (Fig. 4b) $\kappa = (0.615 \pm 0.003) \times (c_{\text{Ni}} - c_f)$, which reflects the decrease in the sizes of the finite clusters with increasing c_{Ni} . The cluster sizes then decrease faster than the increase of $1/\kappa$ in the antiferromagnetic matrix as $c_{\text{Ni}} \rightarrow c_f$.

CONCLUSION

Joint measurements of χ and of $d\sigma/d\Omega$ have made it possible to determine the features of ferromagnetic order evolution and spin-glass formation in high-concentration systems. The appearance of SMSN at $T = 4.2$ K indicates that finite ferromagnetic clusters are produced and the latter form in turn cluster spin glass. This result points also to the coexistence of spin glass and long-range ferromagnetic order at $c_{\text{Ni}} > c_f$ and below T_g .

It appears that owing to the cluster mechanism of spin-glass formation, where an important role is played by the magnetic states of the regions between the clusters, the adjacent states exert a noticeable influence on the value of T_g .

What turns out to be somewhat unexpected is the great similarity between the evolution of ferromagnetism in these complex metallic systems, on the one hand, and percolation processes, on the other. This similarity is possibly due to the cluster mechanism according to which the clusters increase in size mainly on account of exchange interactions of the nearest neighborhoods.

The authors thank I. M. Puzeř, B. N. Mokhov, and A. Z. Men'shikov for a discussion of some of the results.

¹S. L. Ginsburg, Physics of the Condensed State (Proc. 16th School of the Leningrad Inst. of Nucl. Phys), A. I. Okorokov, ed., Leningrad, 1982, p. 43.

²C. M. Hurd, Contemp. Phys. **23**, 469 (1982).

³V. I. Goman'kov, B. N. Mokhov, and N. I. Nogin, Zh. Eksp. Teor. Fiz. **77**, 630 (1979) [Sov. Phys. JETP **50**, 317 (1979)].

⁴A. V. Deryabin, Yu. A. Chirkov, and A. V. T'kov, *ibid.* **86**, 609 (1984) [59, 355 (1984)].

⁵A. Z. Men'shikov, G. A. Takzei, and A. E. Teplykh, Fiz. Met. Metallov. **54**, 465 (1982).

⁶A. P. Murani, Phys. Rev. Lett. **37**, 450 (1976).

⁷Y. Ishikawa, M. Kohgi, Y. Noda, and K. Tajima, Proc. Internat. Conf. on Magnetism, ICM-73 [in Russian], Nauka, 1974, Vo. 4, p. 567.

⁸S. K. Burke and B. D. Rainford, J. Phys. F**13**, 471 (1983).

⁹B. D. Rainford, J. Magnetism and Magnetic Materials **14**, 197 (1979).

¹⁰J. W. Lynn, R. W. Erwin, R. S. Chen, and J. J. Rhyne, Sol. State Comm. **46**, 317 (1983).

¹¹S. K. Burke, R. Cywinski, J. R. Davis, and B. D. Rainford, J. Phys. F**13**, 452 (1983).

¹²M. Takahashi, Digest of Intermag '84, 1984, p. 414.

¹³M. A. Krivoglaz, Dokl. Akad. Nauk SSSR **3**, 61 (1958).

¹⁴J. C. Ododo and B. D. Rainford, J. Phys. C**11**, L533 (1978).

Translated by J. G. Adashko